Available online at www.sciencedirect.com
ScienceDirect
Trans. Nonferrous Met. Soc. China 22(2012) 503−509
Transactions of Nonferrous Metals Society of China
www.tnmsc.cn

Characterization of hot deformation microstructures of alpha−beta titanium alloy with equiaxed structure

CHEN Hui-qin[1], CAO Chun-xiao[2]

1. School of Materials Science and Engineering, Taiyuan University of Science and Technology, Taiyuan 030024, China;
2. Beijing Aeronautical Materials Institute, Aviation Industry Corporation of China (AVIC), Beijing 100095, China

Received 26 April 2011; accepted 2 June 2011

Abstract: Hot deformation behavior and microstructure evolution of TC11 (Ti−6.5Al−3.5Mo−1.5Zr−0.3Si) alloy with equiaxed structure were investigated in the two-phase field at temperatures in the range of 980−800 °C and at strain rates of 0.001 s^{-1}, 0.01 s^{-1}, 0.1 s^{-1}. Effects of thermo-mechanical parameters on both of the stress—strain curves and microstructure evolution were analyzed. Grain boundary characteristics of deformation microstructures were tested by electron backscattered diffraction (EBSD). The results reveal that *β*-phase dominates the deformation and presents discontinuous dynamic recrystallization at 980 °C; meanwhile, *α*-phase coarsens at lower strain rates and dissolves at higher strain rates, and *α*-phase volume fraction and grain size decrease with increasing strain rate. Super-plastic deformation occurs at 950−900 °C and strain rate of 0.001 s^{-1}. And the deformation is dominated by soft *β*-phase, phase interfaces and grain boundaries. Microstructural mechanism operated at 850 °C is continuous dynamic recrystallization of *α*-phase that dominates the deformation, and *β*-phase deforms to match the deformation of *α*-phase.

Key words: TC11 titanium alloy; equiaxed structure; hot deformation; microstructure evolution

1 Introduction

Microstructure plays a very important role in the mechanical properties of alloys. For example, the lamellar microstructure in titanium alloys possess higher creep resistance, fracture toughness and crack propagation resistance, but the equiaxed microstructure has a good combination of strength and ductility [1]. The complex two-phase nature of titanium alloys not only provides a variety of microstructures ranging from the *β*-transformed (martensitic or lamellar) to the equiaxed *α*−*β* microstructure, but also poses many challenges in microstructural control during thermo-mechanical processing to meet final forged component properties [2].

The flow stress data and microstructure observation (OM, SEM and TEM) usually are applied to identifying various microstructural mechanisms that operate under different temperature and strain rate combinations [3,4]. Recently, an approach of processing maps has been developed to optimize workability, control microstructures, and avoid defects for some material systems [5−7]. But electron backscattered diffraction (EBSP) can provide the orientation map of crystallites used to identify regions which may be grains or sub-grains, and has made a possible great leap forward to investigate the grain boundary evolution during recovery and recrystallization [8−10]. Recrystallization is the formation of a new grain structure in a deformed material by the formation and migration of high angle grain boundaries (greater than a 10°−15° misorientation) driven by the stored energy of deformation; and recovery occurs without the migration of a high angle grain boundary [11]. Thereby, discontinuous dynamic recrystallization occurring in alloys with lower stacking fault energy (SFE), such as *γ*-steel, was identified [12]. And geometrical dynamic recrystallization occurs in alloys with higher SFE, such as Al or Zr alloys [13,14].

Microstructure evolution of titanium alloys during hot working is very sensitive to process parameters, such as temperature, strain rate, strain, and “history” of the material (chemistry and starting microstructural condition) [15]. One of the very common industrial

Foundation item: Project (2008011045) supported by the Natural Science Foundation of Shanxi Province, China
Corresponding author: CHEN Hui-qin; Tel: +86-351-6998162; Fax: +86-351-6998277; E-mail: chenhuiqin@tyust.edu.cn
DOI: 10.1016/S1003-6326(11)61205-3

processes is the super-plastic forming generally conducted on the equiaxed structure in the two-phase field of titanium alloys. The super-plastic deformation in Ti−6Al−4V has been studied in Refs. [5−7], and microstructural mechanisms have been identified to be dynamic recrystallization in other reports [16,17]. The present work aims to study microstructural mechanisms of the TC11 alloy with an equiaxed starting microstructure during hot compression in the two-phase field and by EBSD tests.

2 Experimental

TC11 having the following composition (mass fraction, %) was used in the present investigation: 6.42Al, 3.29Mo, 1.79Zr, 0.23Si, 0.025C, 0.077Fe, 0.96O, 0.0044N, 0.0034H and balance Ti. The β transus temperature for this material is about 1008 °C [18]. The starting microstructure shown in Fig. 1 is the perform equiaxed structure.

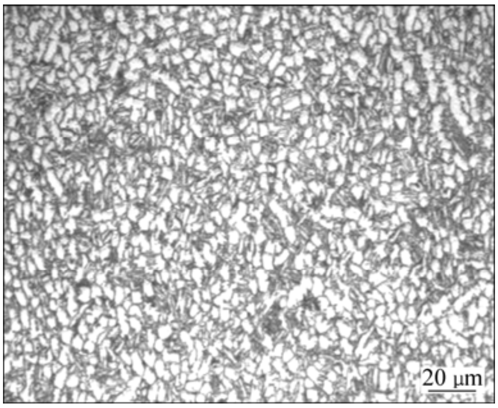

Fig. 1 OM metallographic photo showing starting structure of TC11 alloy

Compression specimens with 12 mm in height and 8 mm in diameter were machined for testing. Concentric grooves with 0.2 mm in depth were made on the top and bottom faces of the specimens to trap lubrication and assist in reducing friction. Thermocouples welded in the middle surface of the specimens were used to measure the actual temperature of the specimens. Isothermal hot compression tests were conducted using a thermecmastor-Z thermo-mechanical simulator at temperatures in the range of 980−800 °C at strain rates of 0.001 s^{-1}, 0.01 s^{-1}, 0.1 s^{-1}. The specimens were deformed to the specified reduction and quenched to freeze microstructure after deformation. The true stress—true plastic strain curves at different temperatures and strain rates were obtained.

Deformed specimens sectioned parallel to the compression axis were prepared for metallographic examination. The microscopy specimens were etched with Kroll’s reagent and optical micrographs were recorded by ZEISS-AXIO. EBSD tests were conducted on TESCAN−5136XM SEM, and scan step was 1 μm for 200×200.

3 Results and discussion

3.1 Flow stress behavior

The typical flow stress curves exhibited by TC11 alloy with the equiaxed starting microstructure are given in Fig. 2, which reveal that the flow stress behavior is different at different strain rates and temperatures. The curve exhibits strain hardening firstly and then reaching the steady state at 0.001 s^{-1} and 950 °C. This kind of

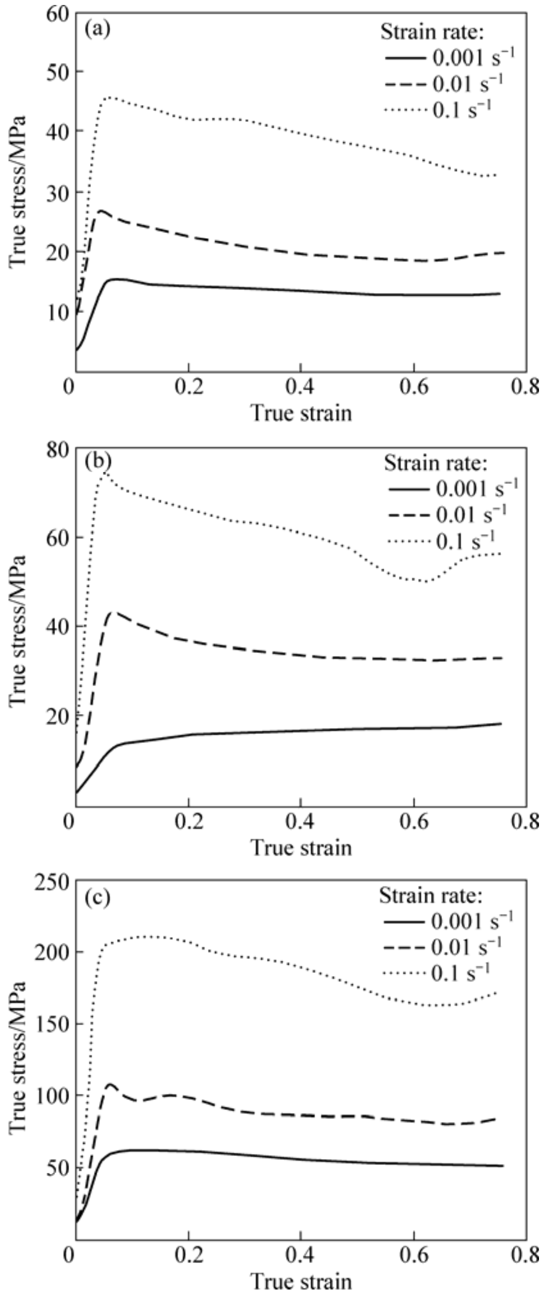

Fig. 2 True stress—strain curves of TC11 alloy at different temperatures: (a) 980 °C; (b) 950 °C; (c) 850 °C

steady-state type curve indicates that the mechanism of softening is sufficiently fast to balance the rate of work hardening and is suggestive of mechanism like dynamic recovery or super-plastic deformation [5−7]. At strain rate of 0.1 s^{-1} and all temperatures, the curves exhibit a broad softening after the first strain hardening, and then reaching the steady state at larger strains, which has been observed for discontinuous dynamic recrystallization of titanium alloys with equiaxed structures [16,17]. At other strain rates and temperatures, the curves exhibit a slight softening after the first strain hardening, and then reaching the steady state quickly. This kind of curve indicates that softening is also sufficiently fast to balance the rate of work hardening, and reach the microstructure state similar to that at 0.001 s^{-1} and 950 °C.

3.2 Kinetic analysis

The temperature and strain rate dependence of flow stress in hot deformation is generally expressed in terms of a kinetic rate equation given by

$$\dot{\varepsilon} = A\sigma^n \exp\left(-\frac{Q}{RT}\right) \tag{1}$$

where $\dot{\varepsilon}$ is the strain rate; σ is the flow stress; A is the material constant; Q is the deformation activation energy; R is the mole gas constant; T is the thermodynamic temperature in Kelvin; n is a stress exponent.

In order to identify the mechanism of hot deformation, the kinetic parameters, n and Q in Eq. (1), are to be evaluated. The variation of peak stresses with strain rates is shown in Fig. 3(a) on a ln σ−ln $\dot{\varepsilon}$ scale. The inverse of the slope of this curve represents the stress exponent, n. From Fig. 3(a), it is seen that n is temperature and strain rate dependent over the entire range in this study, especially at 950 °C, 900 °C and strain rate of 0.001 s^{-1}. Because the strain rate sensitivity index m equals the inverse of n, it is seen obviously in Fig. 3(b) that the strain rate sensitivity indexes at 950 °C, 900 °C and strain rate of 0.001 s^{-1} are much greater than 0.3, others are between 0.3 and 0.15. It is suggestive that the mechanism of deforming at 950 °C, 900 °C and strain rate of 0.001 s^{-1} is super-plastic deformation, and the mechanism of deformation at other parameters in this study is dislocation glide and climb mainly.

The average value of stress exponent, n, is estimated to be about 3.8 over the entire temperature range in this study. The apparent activation energy estimated from Eq. (1) and the average value of stress exponent is 471.6 kJ/mol, which is lower than that in the previous work [18]. The error may come from different specimen sizes and the principle of thermo-simulators. But the two values are both in the reasonable range of 400−600 kJ/mol [19]. This value is much higher than that for self diffusion in α-Ti (150 kJ/mol) and β-Ti (153 kJ/mol) [5−7]. The abnormally high values of the activation energy probably due to the α- and β-phase volume fraction are not constant over the experimental temperature range and Eq. (1) does not include the influence of these factors on deformation kinetics. BRIOTTET et al [19] accounted for the reason of the high activation energy in the two-phase field compared with the activation energies of the constituent phases.

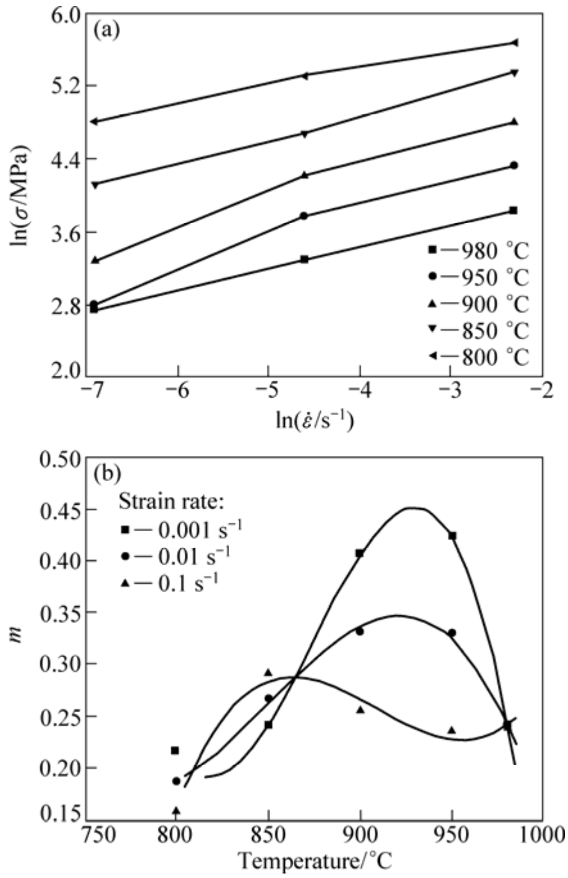

Fig. 3 Variation of peak stress of TC11 with strain rate (a) and variation of strain rate sensitivity index with temperature (b)

3.3 Microstructure observation and characterization

From the above analysis, it is seen that the mechanisms at strain rate of 0.001 s^{-1} may be different at different temperatures in the two-phase field of TC11 alloy. This may be due to the dramatic transformation at strain rate of 0.001 s^{-1}, and the α- and β-phase volume fractions are not constant over the whole experimental temperature range.

The microstructures obtained on the compressed specimens under different temperatures and strain rates were examined, and typical microstructures obtained at a strain rate of 0.001 s^{-1} and different temperatures are shown in Figs. 4−6. From these microstructures, it is seen that the α grain size as well as the α-phase volume fraction decrease with increasing temperature. From these plots, it may be noted also that different microstructure morphologies and grain boundary

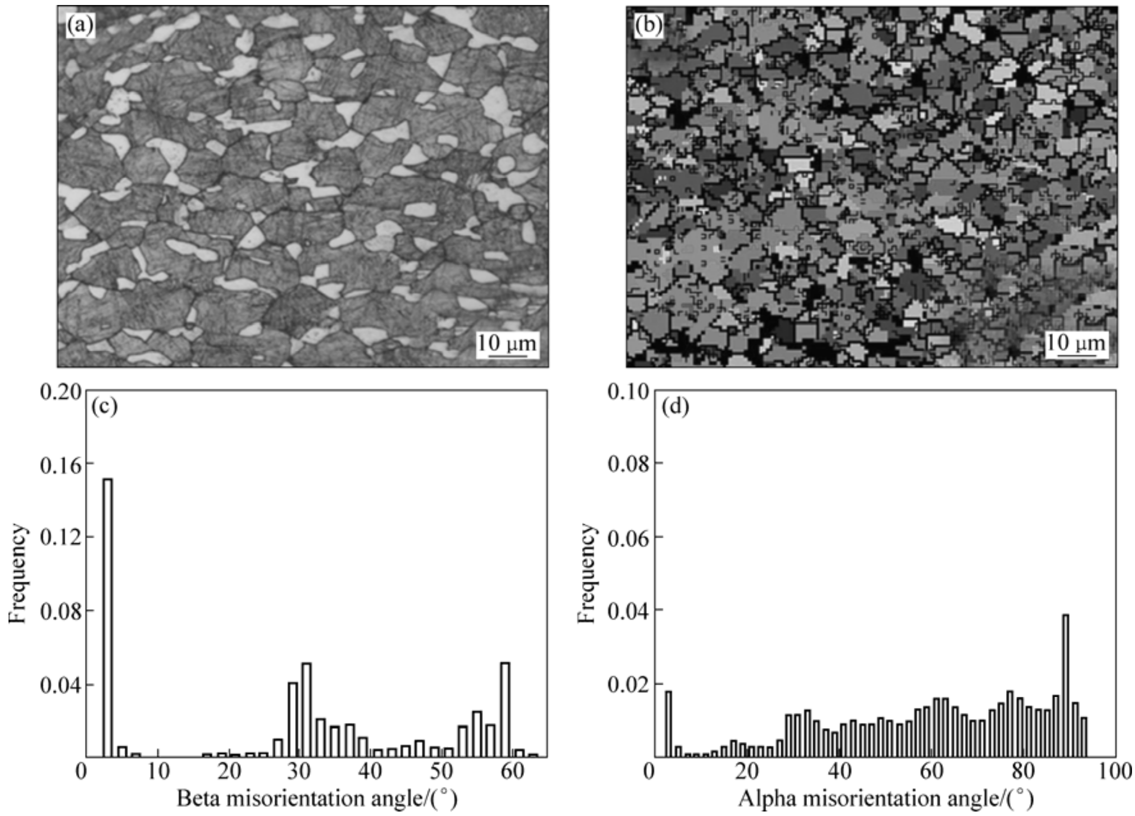

Fig. 4 OM (a), EBSD map (HAGBs shown as thick lines and LAGBs as thin lines) (b), corresponding β-phase misorientation distribution (c) and α-phase misorientation distribution (d) at 980 °C, 0.001 s^{-1} and strain of 0.7

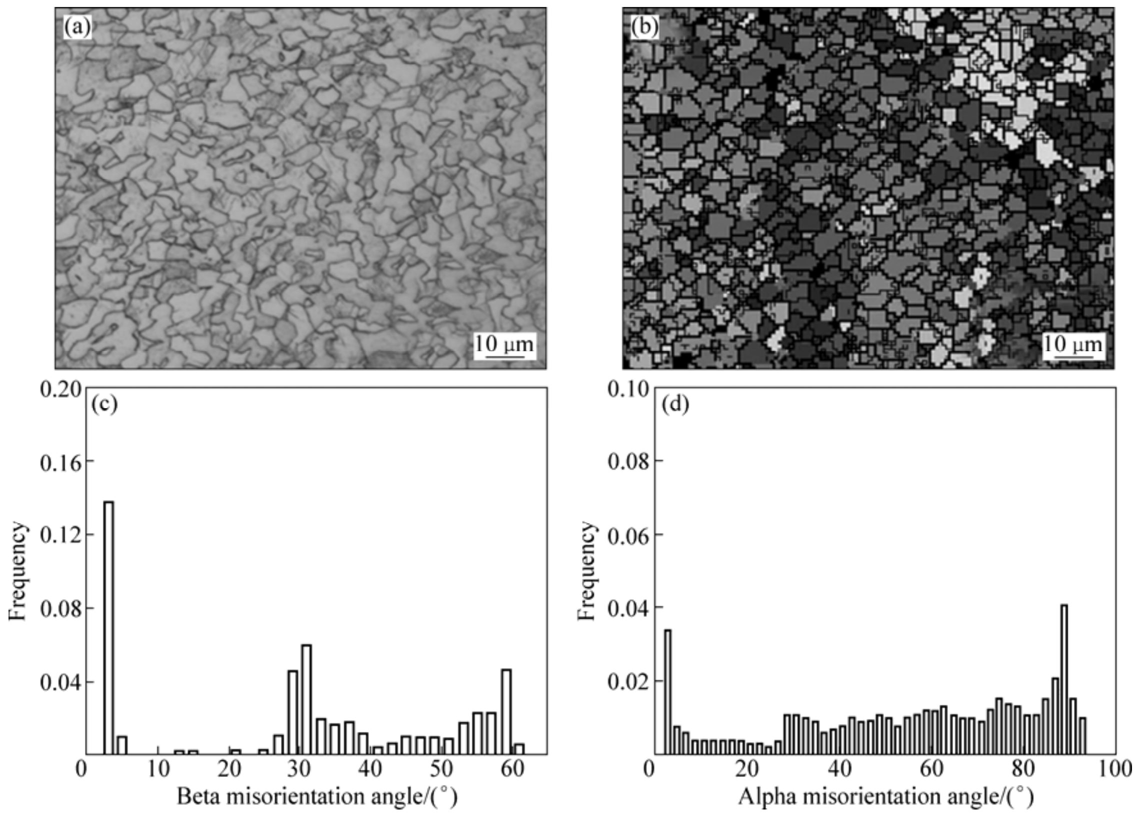

Fig. 5 OM (a), EBSD map (HAGBs shown as thick lines and LAGBs as thin lines) (b), corresponding β-phase misorientation distribution (c) and α-phase misorientation distribution (d) at 950 °C, 0.001 s^{-1} and strain of 0.7

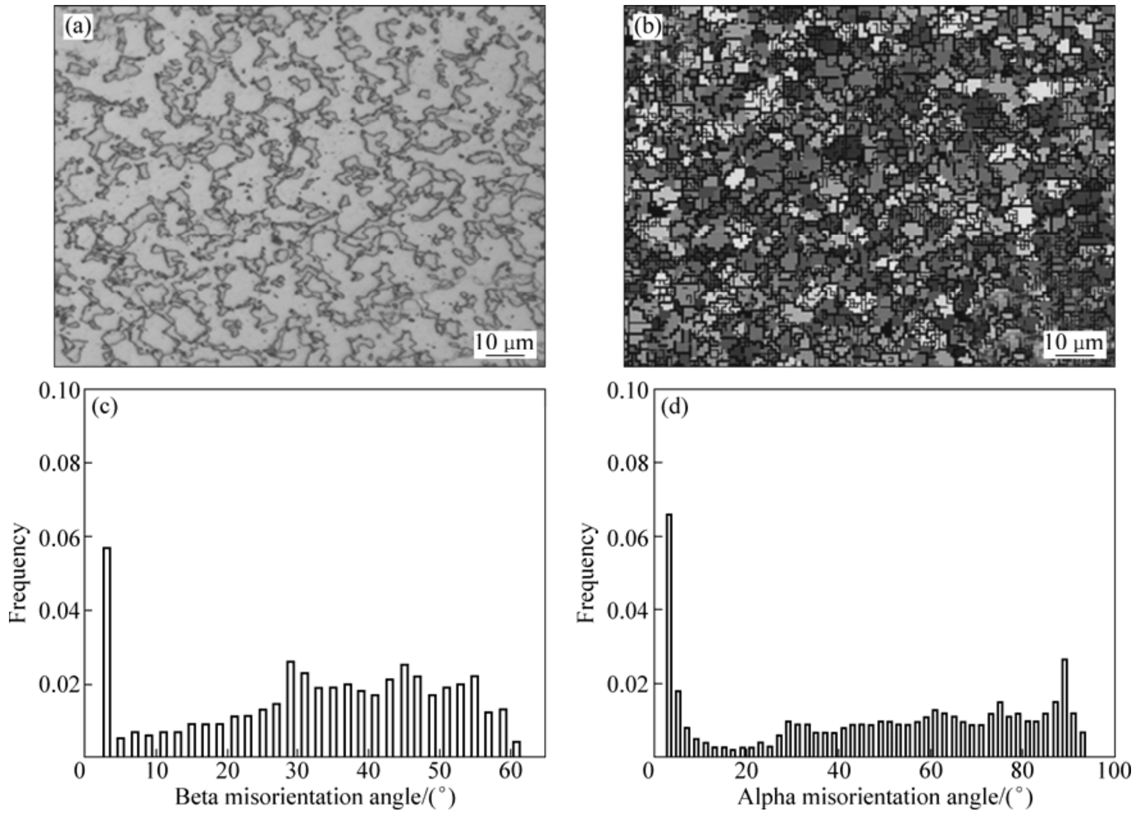

Fig. 6 OM (a), EBSD map (HAGBs shown as thick lines and LAGBs as thin lines) (b), corresponding β-phase misorientation distribution (c) and α-phase misorientation distribution (d) at 850 °C, 0.001 s^{-1} and strain of 0.7

characteristics present at different temperatures under the same deformation strain rate of 0.001 s^{-1}.

As shown in Fig. 4(a), β-phase dominates the microstructure at 980 °C. β grains elongate slightly along the deformation direction. α grains with smooth grain boundaries locate in the triple junction region of β grains. The bimodal distribution of β-phase misorientation in Fig. 4(c) indicates that the transition from low angle grain boundaries (<15°, LAGBs) to high angle grain boundaries (≥15°, HAGBs) is discontinuous, which identifies that discontinuous dynamic recrystallization takes place in β-phase. However, the proportion of low angle grain boundaries is much lower in the misorientation distribution of α-phase (Fig. 4(d)). High angle grain boundaries dominate in α-phase misorientation. This indicates that α-phase presents small deformation, and no recrystallization occurs in α-phase during deformation at 980 °C and 0.001 s^{-1}.

The volume fractions of β-phase and α-phase in microstructures at 950 °C are almost equal (Fig. 5(a)). As shown in Fig. 5(a), microstructure morphology with rough grain boundaries and phase boundaries is irregularity. In general, the rough boundaries possess higher energies, which is the result of deformation along these boundaries. The boundary characteristic of β-phase (Fig. 5(c)) is similar to that at 980 °C. But the boundary characteristic of α-phase (Fig. 5(d)) is different from that at 980 °C. The proportion of lower angle boundaries is higher in α-phase misorientation, and the frequency of lower angle boundaries is uniform (Fig. 5(d)). This characteristic of α-phase misorientation distribution indicates that lower angle boundaries after the first strain hardening on the flow stress curve became dynamic stable, and induced the steady state type flow stress curve. Based on the characteristic of α-phase misorientation distribution and the value of strain rate sensitivity index in Fig. 3(b), it is identified that the super-plastic deformation takes place at 950 °C and 0.001 s^{-1}, which is in agreement with the result in the previous work [18]. The super-plastic properties of titanium alpha/beta alloys are a result of the fine, two-phase microstructure of equiaxed alpha and beta grains (Fig. 5(a)). At strain rate of 0.001 s^{-1}, the microstructure deforms by diffusion controlling, grain boundary sliding thus giving rise to stable low angle boundaries (Fig. 5(d)) and high value of the strain rate sensitivity index m (Fig. 3(b)) as well as deformed microstructures which retain much of their original equiaxed nature (Fig. 5(b)). The presence of two phases helps to limit the growth of either to large extent, thereby enabling the retention of the plastic properties to large strains.

At 850 °C, α-phase dominates the microstructure (Fig. 6(a)). The transition from low angle grain boundaries to high angle boundaries in α-phase misorientation of Fig. 6(d) is continuous, which indicates that continuous dynamic recrystallization takes place in α-phase. But the volume fraction of β-phase in microstructures at 850 °C is much lower than that of α-phase (Fig. 6(a)). As shown in Fig. 6(c), the proportion of lower angle boundaries in the misorientation distribution of β-phase is much lower, and high angle boundaries dominate in β-phase misorientation. These indicate that β-phase is not the dominated deformation phase at 850 °C, and no recrystallization occurs in β-phase also. Due to the irregularity morphology of microstructure and rough grain boundary and phase boundary, β-phase presents deformation to match the deformation of α-phase.

Because of transformation in the two-phase field, the volume fractions of α- and β-phases vary with temperatures. Therefore, the flow stress behavior and mechanism of hot deformation at different temperatures are different, that is, transformation has influence on deformation of TC11 alloy in the two-phase field, vice versa, deformation can influence transformation, especially at 980 °C. Microstructures deformed to the strain of 0.7 at 980 °C and different strain rates are shown in Fig. 7. It is seen that the volume fraction and grain size of α-phase decrease with increasing strain rate, that is, α-phase dissolves at higher strain rates, and coarsens at lower strain rates during deformation at 980 °C and 0.001 s^{-1}.

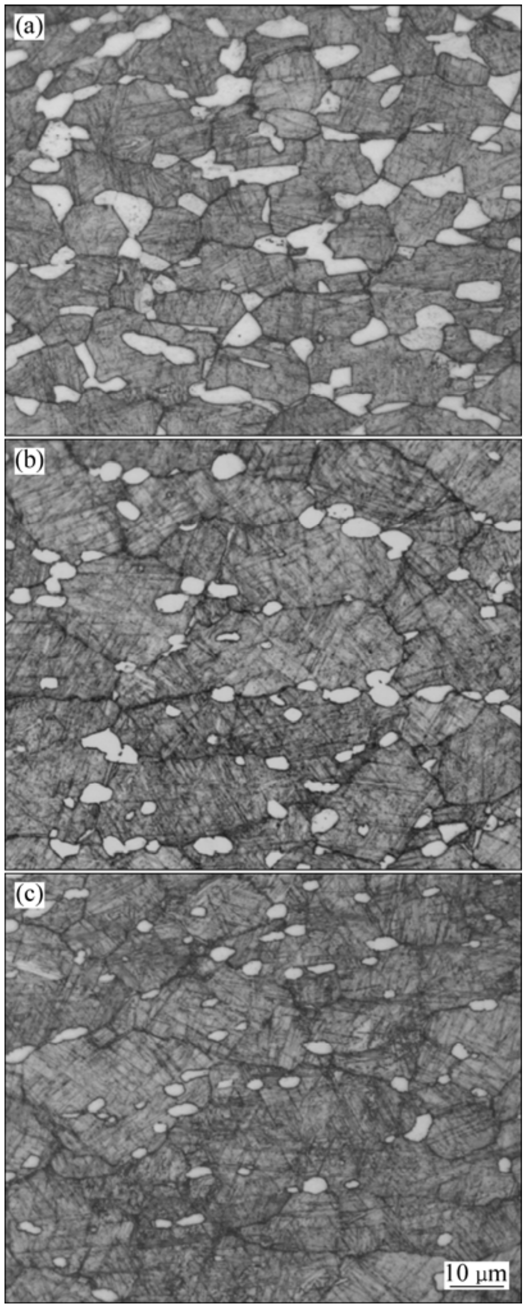

Fig. 7 Deformation microstructures at 980 °C and strain of 0.7 and different strain rates: (a) 0.001 s^{-1}; (b) 0.01 s^{-1}; (c) 0. 1 s^{-1}

4 Conclusions

1) Because of transformation, hot deformation behavior and microstructure evolution of TC11 alloy with equiaxed structure in the two-phase field vary with deformation temperature and strain rate.

2) The mechanism of deformation at 950 °C, 900 °C and strain rate of 0.001 s^{-1} is super-plastic deformation; the mechanism of deformation at other temperatures and strain rates in this study is dislocation glide and climb mainly.

3) β-phase dominates the deformation and presents discontinuous dynamic recrystallization at 980 °C. Meanwhile, α-phase coarsens at lower strain rates and dissolves at higher strain rates, and α-phase grain size and volume fraction decrease with increasing strain rate.

4) During super-plastic deformation process, the deformation occurs in soft β-phase, at phase interfaces and grain boundaries mainly.

5) Microstructural mechanism operated at 850 °C is continuous dynamic recrystallization occurring in α-phase that dominates the deformation and β-phase deforms to match the deformation of α-phase.

References

[1] SEMIATIN S L, SEELHARAMAN V, WEISS I. Hot working of titanium alloys—An overview [C]//WEISS I. Advances in the Science and Technology of Titanium Alloy Processing. Warrendale: The Minerals, Metals & Materials Society, 1997: 3−37.

[2] SHEN G, FURRER D, ROLLIONS J. Microstructural development in a titanium alloy [C]//WEISS I. Advances in the Science and Technology of Titanium Alloy Processing. Warrendale: The Minerals, Metals & Materials Society, 1997: 75−82.

[3] MCQUEEN H J. Interpretation of microstructures in high temperature deformation [C]//Advanced Materials for the 21st Century. CHUNG Y W. Weertman: The Minerals, Metals & Materials Society, 1999: 159−168.

[4] MCQUEEN H J, RYAN N D. Constitutive analysis in hot working [J]. Materials Science and Engineering A, 2002, 322: 43−63.
[5] PRASAD Y V R K, SESHACHARYULU T. Processing maps for hot working of titanium alloy [J]. Materials Science and Engineering A, 1998, 243: 82−88.
[6] SESHACHARYULU T, MEDEIROS S C, FRAZIER W G, PRASAD Y V R K. Hot working of commercial Ti−6Al−4V with an equiaxed *α*−*β* microstructure: Materials modeling consideration [J]. Materials Science and Engineering A, 2000, 284: 184−194.
[7] PRASAD Y V R K, SESHACHARYULU T, MEDEIROS S C, FRAZIER W G. Influence of oxygen content on the forging response of equiaxed (*α*+*β*) preform of Ti−6Al−4V: commercial vs. ELI grade [J]. Journal of Materials Processing Technology, 2001, 108: 320−327.
[8] JENSEN D J. Deformation and recrystallisation studied by EBSP: Breakthroughs and limitations [J]. Materials Science and Technology, 2000, 16(11−12): 1360−1363.
[9] SALISHCHEV G A, ZEREBTSOV S V, MIRONOV S Y U, SEMIATIN S L. Formation of grain boundary misorientation spectrum in alpha-beta titanium alloys with lamellar structure under warm and hot working [J]. Materials Science Forum, 2004, 467−470: 501−506.
[10] FURUHARA T, POORGANJI B, ABE H, MAKI T. Dynamic recovery and recrystallization in titanium alloys by hot deformation [J]. JOM, 2007(1): 64−67.
[11] DOHERTY R D, HUGHES D A, HUMPHREYS F J, JONAS J J, JUUL JENSEN D, KASSNER M E, KING W E, MCNELLEY T R, MCQUEEN H J, ROLLETT A D. Current issues in recrystallization: A review [J]. Materials Science and Engineering A, 1997, 238: 219−274.
[12] HUMPHREYS F J, HATHERLY M. Recrystallization and related annealing phenomena [M]. Oxford: Elsevier, 2004.
[13] BARRABES S R, KASSNER M E, PEREZ-PRADO M T, EVANGELISTA E. Geometric dynamic recrystallization in *α*-zirconium at elevated temperature [J]. Materials Science Forum, 2004, 467−470: 1145−1150.
[14] KAIBYSHEV R, MAZURINA I, SITDIKOV O. Geometric dynamic recrystallization in an AA2219 alloy deformed to large strains at an elevated temperature [J]. Materials Science Forum, 2004, 467/470: 1199−1204.
[15] JACKSONA M, JONESB N G, DYEB D, DASHWOODC R J. Effect of initial microstructure on plastic flow behaviour during isothermal forging of Ti−10V−2Fe−3Al [J]. Materials Science and Engineering A, 2009, 501: 248−254.
[16] HUANG, L J, GRNG L, LI A B, CUI X P, LI H Z, WANG G S. Characteristics of hot compression behavior of Ti−6.5Al−3.5Mo−1.5Zr−0.3Si alloy with an equiaxed microstructure [J]. Materials Science and Engineering A, 2009, 505: 136−143.
[17] ZONG Y Y, SHAN D B, XU M, LU Y. Flow softening and microstructural evolution of TC11 titanium alloy during hot deformation [J]. Journal of Materials Processing Technology, 2009, 209: 1988−1994.
[18] CHEN H Q, LIN H Z, GUO L, CAO C X. Hot deformation behavior and microstructure evolution of Ti−6.5Al−1.5Zr−3.5Mo−0.3Si with an equiaxed *α*+*β* starting structure [J]. Materials Science Forum, 2007, 546−549: 1383−1388.
[19] BRIOTTET L, JONAS J J, MONTHEILLET F. A mechanical interpretation of the activation energy of high temperature deformation in two phase materials [J]. Acta Materialia, 1996, 44(4): 1665−1672,

等轴组织 *α*–*β* 钛合金热变形微观组织的表征

陈慧琴[1]，曹春晓[2]

1. 太原科技大学 材料科学与工程学院，太原 030024；
2. 中国航空工业 北京航空材料研究院，北京 100095

摘　要：研究等轴组织 TC11(Ti−6.5Al−3.5Mo−1.5Zr−0.3Si)合金在两相区 980~800 °C 温度范围和应变速率 0.001 s^{-1}，0.01 s^{-1}，0.1 s^{-1} 条件下的热变形行为和微观组织演变。分析热力模拟参数对应力—应变曲线和微观组织演变的影响。并采用电子背散射衍射(EBSD)技术测试表征变形组织的晶界特征。研究结果表明：在 980 °C 变形时，*β* 相是主要变形相，发生了不连续动态再结晶；同时，*α* 相经历了变形促进下的聚集粗化(低应变速率)和溶解(高应变速率)的过程，即 *α* 相含量和晶粒尺寸随着应变速率的加快而明显减小。在 950~900 °C，0.001 s^{-1} 应变速率的条件下发生超塑性变形时，变形主要集中在软的 *β* 相，以及相界和晶界处。在 850 °C 时，*α* 相是主变形相，变形微观组织的演变机理是 *α* 相的连续动态再结晶，*β* 相起晶界协调变形的作用。

关键词：TC11 钛合金；等轴组织；热变形；微观组织演变

(Edited by YANG Hua)